Proceedings of Institute of Mathematics of NAS of Ukraine 2000, Vol. 30, Part 1, 239–244.

On Invariant Wave Patterns in Non-Local Model of Structured Media

V.A. VLADIMIROV and S.I. SKURATIVSKY

Division of Geodynamics of Explosion, Subbotin Institute of Geophysics, NAS of Ukraine, Khmelnicki Str. 63-B, Kyiv 54, Ukraine
E-mail: vsan@ambernet.kiev.ua

A set of invariant solutions of a modelling system describing long nonlinear waves propagation in medium with internal structure is considered. Using the well known symmetry reduction method we perform transition from the initial system of PDE to a third-order dynamical system. Employing the qualitative theory method as well as direct numerical simulation, we study forms of multiperiodic, quasiperiodic, chaotic and soliton-like invariant solutions. Parametric portraits are presented and the structure of a set of parameters corresponding to the soliton-like solutions is analyzed. Within the method applied it manifests fractal features.

It is well known, that most of the earth materials possess internal structure. Such are rocks, soils, layered media and lithosphere itself. Such are a lot of artificial substances – concrete, air-liquid mixtures, polymers and so on. When studying high-speed high-intense loading afteractions in structured media the problem of their adequate description arises, since continual approach in such circumstances is not valid and integro-differential relations must be used [1]. Such relations are not easy to deal with and, besides, they contain, as a rule, unknown kernels of relaxations [1] that must be determined in every particular case.

It turns out that knowledge of details of the relaxing mechanisms is almost unnecessary if the processes to be described are weakly non-equilibrium, which is the case when we restrict to the consideration of the long waves propagation. Analysis performed within the asymptotic approach in paper [2] shows that the balance equations for mass and momentum in the long wave limit do not depend on structure, retaining their classical form. So all the information about the structure in this approximation should be concentrated in the dynamical equation of state (DES) which may be obtained using the methods of phenomenological thermodynamics of non-equilibrium processes. Here we employ the DES, which describes relaxing effects, as well as purely spatial non-locality [3]. Together with balance equations for mass and momentum taken in the hydrodynamic approximation, it forms a closed system of the following form:

$$\begin{aligned} &\frac{d\rho}{dt}+\rho\frac{\partial u}{\partial x}=0, \qquad \rho\frac{du}{dt}+\frac{\partial p}{\partial x}=\gamma\rho, \\ &\tau\left(\frac{dp}{dt}-\chi\frac{d\rho}{dt}\right)=\kappa\rho-p+\sigma\left\{\frac{\partial^2 p}{\partial x^2}+\frac{1}{\rho}\frac{\partial p}{\partial x}\frac{\partial \rho}{\partial x}-\chi\left(\frac{\partial^2\rho}{\partial x^2}-\frac{1}{\rho}\left(\frac{\partial\rho}{\partial x}\right)^2\right)\right\}, \end{aligned} \tag{1}$$

where p is pressure, ρ is density, u is the mass velocity, $d(\cdot)/dt=\partial(\cdot)/\partial t+u\partial(\cdot)/\partial x$ is substantial derivative with respect to time, $\rho\gamma$ is the mass force, κ is equal to the square of equilibrium (low-frequency) sound velocity, τ is the time of relaxation, χ is equal to the square of frozen (high-frequency) sound velocity, σ defines the effective range of non-local effects. System (1) describes long non-linear waves evolution in structured media. In this work we present some results concerning the features of a set of travelling wave solutions of this system.

It is easy to prove that system (1) admits a one-parameter group generated by the operator

$$\hat{X} = \frac{\partial}{\partial t} + D\frac{\partial}{\partial x} + \xi\left(\rho\frac{\partial}{\partial \rho} + p\frac{\partial}{\partial p}\right). \tag{2}$$

Using invariants of this operator, obtained with the help of standard technique [4], one is able to construct the ansatz

$$\begin{aligned} &u = U(\omega) + D, \qquad \omega = x - Dt, \\ &\rho = \exp[\xi t + S(\omega)], \qquad p = \rho Z(\omega), \end{aligned} \tag{3}$$

describing a travelling wave moving with constant velocity D (the meaning of the parameter ξ will be explained later on). We are going to show that the set (3) contains periodic, quasiperiodic, multiperiodic, stochastic and soliton-like solutions. The last regime is analyzed in more detail, in particular, a set of parameter space $\left(D^2, \kappa\right)$, for which solitary wave solutions do exist is studied.

Inserting (3) into (1) we obtain an ODE cyclic with respect to the variable S. Functions U, Z and $W = dU/d\omega \equiv \dot{U}$ satisfy the following dynamical system:

$$\begin{aligned} &U\frac{dU}{d\omega} = UW, \qquad U\frac{dZ}{d\omega} = \gamma U + \xi Z + W(Z - U^2), \\ &U\frac{dW}{d\omega} = \left\{U^2\left(\gamma U + \xi Z - WU^2 + \chi\tau W + Z - \kappa\right)\right. \\ &\qquad \left. +\sigma\left\{\left[(\xi + W)(2U(\gamma - UW) + \chi W) + (UW)^2\right]\right\}\right\}\left[\sigma\left(\chi - U^2\right)\right]^{-1}. \end{aligned} \tag{4}$$

Analysis shows that system (4) possesses only one critical point belonging to the physical parameter's range. If $\gamma = \xi Z_0/D$ then this point, having the coordinates

$$U_0 = -D, \qquad Z_0 = \frac{\kappa}{[1 - 2\sigma(\xi/D)^2]}, \qquad W_0 = 0, \tag{5}$$

defines a stationary solution

$$u = 0, \qquad \rho = \rho_0 \exp\left[\frac{\xi x}{D}\right], \qquad p = Z_0\rho,$$

belonging to the set (3). One immediately concludes from the above formula that ξ defines an inclination of inhomogeneity of this solution if the rest of the parameters are fixed.

We begin our study of patterns formation from some analytical estimations, enabling to state the conditions leading to the limiting cycle appearance in vicinity of critical point (5). It is more convenient to work in the coordinate system $X = U + D$, $Y = Z - Z_0$, W, having the origin at the critical point (5), so we rewrite the linear part of system (4) in this reference frame:

$$U\frac{d}{d\omega}\begin{pmatrix} X \\ Y \\ W \end{pmatrix} = \hat{M}\begin{pmatrix} X \\ Y \\ W \end{pmatrix} + o\left(|X, Y, W|\right), \tag{6}$$

where

$$\hat{M} = \begin{pmatrix} 0 & 0 & -D \\ \gamma & \xi & \Delta \\ A & B & C \end{pmatrix}, \qquad A = \frac{\kappa\xi D(2\xi\sigma - \tau D^2)}{Q\sigma(2\sigma\xi^2 - D^2)}, \qquad B = \frac{D^2(1 + \xi\tau)}{Q},$$

$$Q = \sigma(\chi - D^2), \qquad C = Q^{-1}\left\{\xi\sigma\left(\chi - 2D^2\right) - \frac{2D^2\xi\sigma\kappa}{D^2 - 2\sigma\xi^2} + \tau D^2\left(\chi - D^2\right)\right\}.$$

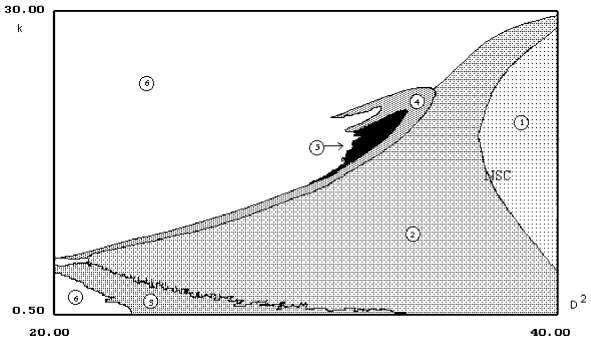

Fig 1. Bifurcation diagram of system (4) in parametric space (D^2, κ): 1 – stable focus; 2 – 1T-cycle; 3 – torus; 4 – multiperiodic attractor; 5 – chaotic attractor; 6 – lose of stability.

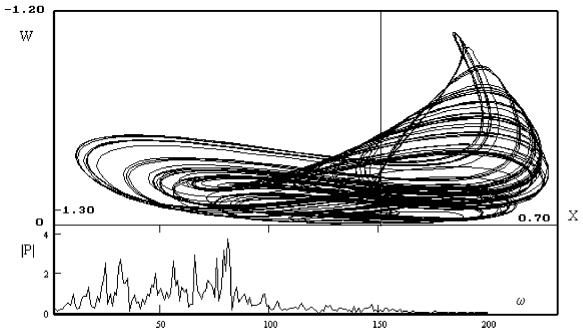

Fig 2. Phase portrait (above) and Fourier spectrum (below) of chaotic solution of system (4) obtained at $\kappa = 17$ and $D^2 = 32.3$.

Let us formulate conditions leading to the appearence of periodic solutions of system (4). According the Hopf theorem [5], limiting cycle is created when a pair of complex conjugate eigenvalues of the matrix $\hat{M}$ crosses the imaginary axis and the third eigenvalue is strictly negative. This is so if the following relations hold:

$$\alpha = \xi + C > 0, \tag{7}$$

$$\Omega^2 = AD - B\Delta + \xi C > 0, \tag{8}$$

$$\alpha\Omega^2 = \xi(AD - Z_0 B). \tag{9}$$

The first two of them take on the form of inequalities, imposing some restrictions on the parameters, while the third one determines the neutral stability curve (NSC) in the plane (κ, D^2), providing that the rest of parameters are fixed. If $\sigma = 0.76$, $\tau = 0.1$, $\chi = 50$, $\xi = 1.8$ then the NSC looks like a parabola with branches directed from right to left. It is presented on Fig. 1 as a bold line.

Numerical investigations illustrated by Fig. 1 show that inside the parabola the critical point $A(-D, Z_0, 0)$ is a stable focus. When we cross the neutral stability curve (9) from right to left, then the stable periodic solution softly appears. The radius of the limiting cycle grows as one goes away from the curve, until it remains stable. Further evolution of periodic regime depends strongly on the values of parameter κ. For $\kappa > 20$ the amplitude of oscilations grows up as the parameter D^2 decreases, till the domain is attained where the regimes become completely unstable.

If the κ lies betwen 10 and 20, then scenario of the development of oscilations is as follows: limiting cycle $\rightarrow$ finite period doubling cascade $\rightarrow \ \cdots \ \rightarrow$ chaotic attractor $\rightarrow$ global lose of stability or falling onto the separated regime existing simultaneously with the main cascade. A typical phase portrait of the regime arising as a result of period doubling cascade is presented on the Fig. 2. Fourier spectrum of X-coordinate, shown on the lower part of Fig. 2, looks like a continious function, so we really deal with the chaotic solutions in this domain of parameters' values.

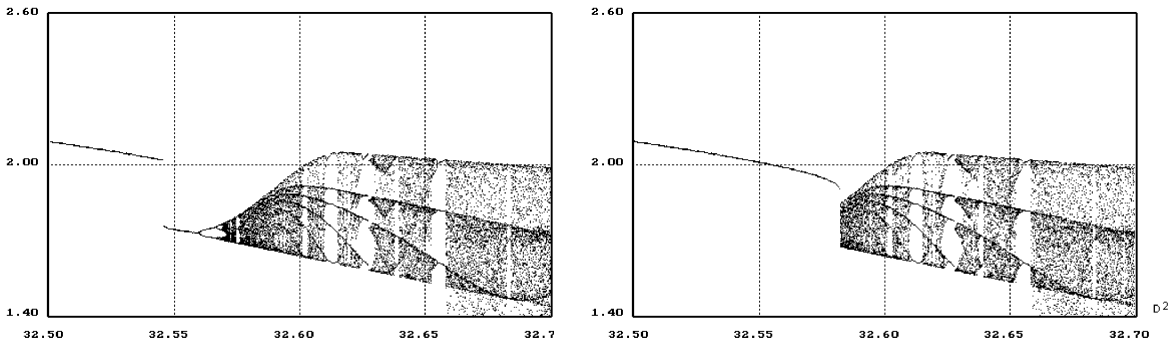

Fig 3. Poincaré sections obtained for $\kappa = 17.82$ when D^2 is decreasing (left) and when D^2 is growing up (right).

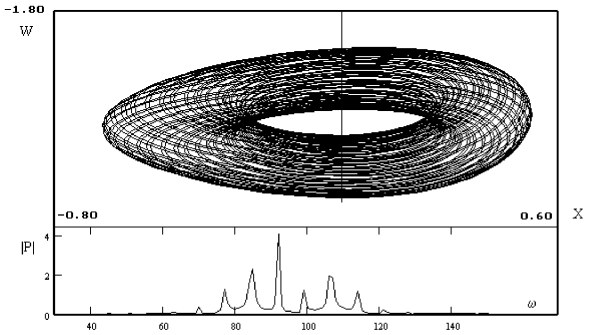

Fig 4. Phase portrait (above) and Fourier spectrum (below) of toroidal attractor of system (4), obtained at $\kappa = 1$ and $D^2 = 24.2$.

In order to study a fine structure of the strange attractor the Poincare sections technique was used [5, 6]. A section plain transversal to the phase traejectories was defined by equation $W = 0$. The bifurcation diagrams shown on Fig. 3 were formed in the following way: we took X coordinates of the points of intersection of the phase trajectories with the plane $W = 0$ and set them on the vertical axis, whereas the corresponding values of the bifurcation parameter D^2 on the horizontal one. Complete list of bifurcation diagrams obtained this way is published in [7]. The most interesting features of system (4) seen on Fig. 3 are the phenomenon of hysteresis and coexistence of different regimes in certain domains of parameters' values.

When $\kappa < 10$, the scenario of the oscillationg regimes development is provided with quasiperiodic solutions and spiral attractors of Šilnikov type [8]. Creation of spiral attractors takes place at the point of intersection of NSC with the horizontal axis, where the linearization matrix $\hat{M}$ has one zero and two pure imaginary eigenvalues. This may be shown explicitely by studying canonical Poincaré form [5] of system (4):

$$\dot{r} = a_1 r y, \qquad \dot{y} = b_1 r^2, \tag{10}$$

where $a_1 = -\frac{D^3\tau}{Q}$, $b_1 = \frac{(\omega^2+\xi^2)\sigma\xi\chi}{DQ\omega^2}$.

A simple analysis shows that system (10) has a center and there arises a stable focus, corresponding to a spiral attractor of system (4), in the domain $r > 0$ when κ is small and positive. The spiral attractor transforms into the isolated regime, existing simultaneously with the main cascade and visible on some of the bifurcation diagrams presented in [7], as the parameter κ sufficiently grows, but in proximity of the horizontal axis it turns into the stable torus when D^2 goes sufficiently far away of the point of NSC intersection with axis. A typical phase portrait of the toroidal regime is shown on Fig. 4. The corresponding Fourier spectrum, shown below the phase portrait, evidently contains maxima defining main frequencies of this quasiperiodic regime.

As it was allready mentioned, system (4) possesses selected regimes, coexisting with the oscillating solutions from the main bifurcation cascade. For certain values of the parameters the

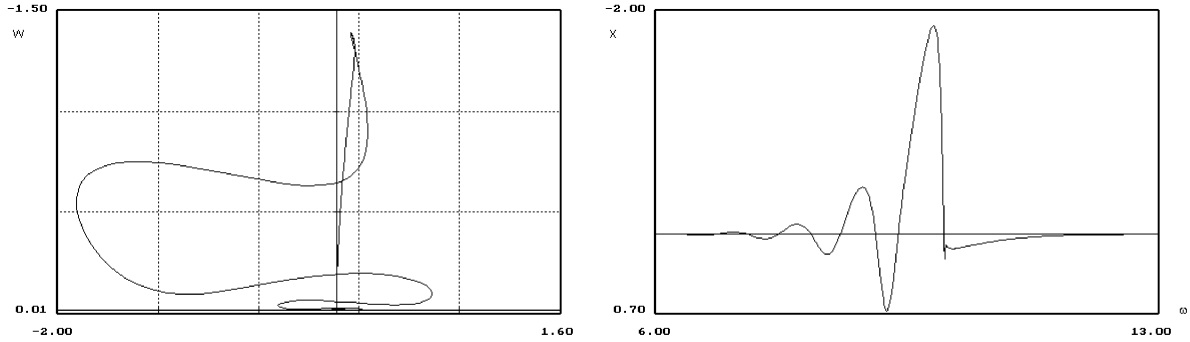

Fig 5. Phase portrit of the soliton-like solution (left) and coordinate U versus ω (right).

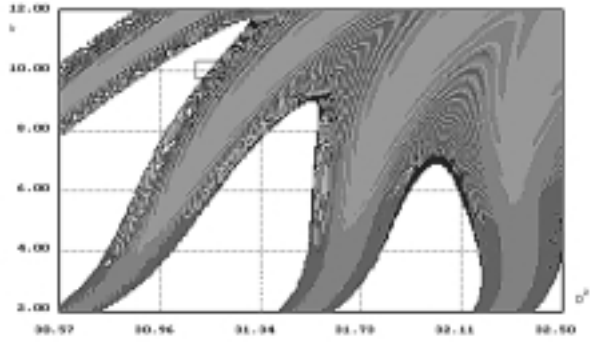

Fig 6. A portrait of subsets of parameter space (D^2, κ), corresponding to different intervals of the function $f^{\Gamma}_{\min}(\kappa, D^2)$ values: $f^{\Gamma}_{\min} > 1.2$ for white colour; $0.6 < f^{\Gamma}_{\min} \leq 1.2$ for light grey; $0.3 < f^{\Gamma}_{\min} \leq 0.6$ for grey; $0.01 < f^{\Gamma}_{\min} \leq 0.3$ for deep grey; $f^{\Gamma}_{\min} \leq 0.01$ for black colour.

isolated regime forms the homoclinic loop, which may be calculated numerically by means of the special technique (Fig. 5). Existence of homoclinic loops among the solutions of system (4) is a very important fact, because these regimes correspond to solitary-wave solutions of the initial PDE system. Therefore we investigate a set of points of paremeter space $\left(D^2, \kappa\right)$, for which trajectories going out of the origin along the one-dimensional unstable invariant manifold W^u return to the origin along the two-dimensional stable invariant manifold W^s. In practice, for a given values of the parameters κ, D^2, we define numerically a distance between the origin and the point $\left(X^{\Gamma}(\omega), Y^{\Gamma}(\omega), W^{\Gamma}(\omega)\right)$ of the phase trajectory $\Gamma\left(\cdot; \kappa, D^2\right)$:

$$f^{\Gamma}\left(\kappa, D^2; \omega\right) = \sqrt{\left[X^{\Gamma}(\omega)\right]^2 + \left[Y^{\Gamma}(\omega)\right]^2 + \left[W^{\Gamma}(\omega)\right]^2}, \tag{11}$$

starting from the fixed Cauchy data. Next we determine minimum $f^{\Gamma}_{\min}(\kappa, D^2)$ of the function (11) for that part of the trajectory that lies beyond the point at which the distance gains its first local maximum, providing that it still lies inside the ball centered at the origin and having a fixed (sufficiently large) radius. The results are presented on Figs. 6–8. First of them is of the most rough scale among this series. Here white colour marks values of the parameters κ, D^2 for which $f^{\Gamma}_{\min} > 1.2$, light gray corresponds to the cases when $0.9 < f^{\Gamma}_{\min} < 1.2$ and so on (further explanations are given in the subsequent captions). The black coloured patches correspond to the case when $f^{\Gamma}_{\min} < 0.03$. Fig. 7 presents the enlargement of the rectangle shown in Fig. 6, whereas Fig. 8 – the enlargement of the rectangle from the Fig. 7. Note, that colours in the last one are re-scaled so e.g. the black colour corresponds to the points at which $f^{\Gamma}_{\min} < 0.003$.

Conclusion

Thus, the modeling system (1), describing media with memory and spatial non-locality possesses a set of complicated invariant solutions, which are effectively investigated with the help of qualitative methods as well as numerical simulation. It is stated the existence of tori and spiral

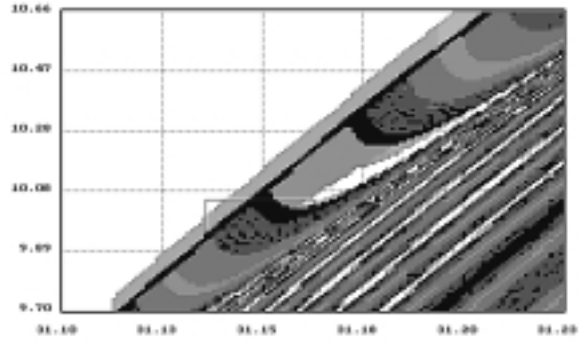

Fig 7. Enlargement of the part of Fig. 6, lying inside the rectangle.

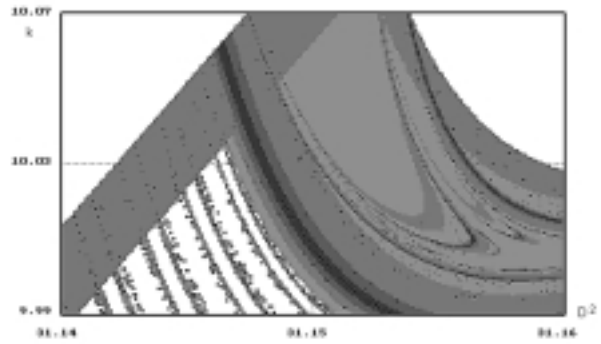

Fig 8. Enlargement of the part of Fig. 7, lying inside the rectangle: $f^{\Gamma}_{\min} > 0.011$ for white colour; $0.007 < f^{\Gamma}_{\min} \leq 0.011$ for light grey; $0.005 < f^{\Gamma}_{\min} \leq 0.007$ for grey; $0.003 < f^{\Gamma}_{\min} \leq 0.005$ for deep grey; $f^{\Gamma}_{\min} \leq 0.003$ for black colour.

attractors of Šilnikov type appearing at the point of parametric space $\left(D^2, \kappa\right)$, corresponding to the doubly degeneracy of the linearized system. The last regime coexists with the main bifurcation cascade (including multiperiodic and chaotic oscillations) and causes hysteretic features of the system. Besides, it gives rise to saddle loops, corresponding to soliton-like solutions of system (1). Numerical investigations show that there are domains of parameter space $\left(D^2, \kappa\right)$ where the soliton-like solutions are not observed and there are domains where the points $\left(D^2, \kappa\right)$, corresponding to the homoclinic loops form dense sets. Within the numerical algorithm applied, the set of points corresponding to the homoclinic solutions manifests fractal features.

It is worth noting that soliton-like solutions of system (1) do not have the classical bell shape. They possess, as a rule, many humps and oscillating tails. Compact wave perturbations of this sort are rather typical to the media with internal structure. One such pulse was created during the Great Chilean Earthquake as it was shown in paper [9]. Another examples may be seen in papers dealing with the models of block geophysical media [10].

References

[1] Rudyak V.Ya., Statistical Theory of Dissipative Processes in Gases and Liquids, Novosibirsk, Nauka, 1987 (in Russian).

[2] Vakhnenko V.A. and Kulich V.V., *J. Appl. Mech. Tech. Phys.*, 1992, V.32, 814–821.

[3] Danevich T.B. and Danylenko V.A., *Proc. of NAS of Ukraine*, 1998, N 10, 133–137 (in Ukrainian).

[4] Ovsyannikov L.V., Group Analysis of Differential Equations, New York, Academic Press, 1982.

[5] Guckenheimer J. and Holmes P., Nonlinear Oscillations, Dynamical Systems and Bifurcations of Vector Fields, New York, Springer, 1987.

[6] Schuster H.G., Deterministic Chaos. An Introduction, Weinheim, Physik-Verlag, 1984.

[7] Vladimirov V.A., Sidorets V.N. and Skurativsky S.I., *Rep. Math. Phys.*, 1999, V.44, N 1–2, 275–282.

[8] Ovsyannikov I.M. and Šilnikov L.P., *Mat. Sbornik*, 1986, V.130 (172), 552–570 (in Russian).

[9] Lund P., *Pure & Appl.Geophys*, 1982, V.1, 121–131.

[10] Starostenko V.I., Danylenko V.A. and Vengrovich D.B., *Tectonophysics*, 1996, V.268, 211–220.